Performance Analysis of Energy Beamforming over Line-of-sight Links

Danyang Wang, *Student Member, IEEE* and Chintha Tellambura, *Fellow, IEEE*
Department of Electrical and Computer Engineering, University of Alberta, Edmonton, Alberta, Canada
Email: danyang5@ualberta.ca, ct4@ualberta.ca

***Abstract*—Performance analysis of energy beamforming with a multiple-antenna access point (AP) and a single-antenna user over line-of-sight (LOS) channels is not readily available. In this paper, we thus consider Rician channels between the AP and the user and derive the distribution of the received signal-to-noise ratio (SNR) via the distribution of the product of two independent non-central Chi-square variables. We also derive exact expressions for outage probability (OP), ergodic capacity (EC), throughput optimal energy harvesting time and bit error rates (BERs). Several approximate or asymptotic expressions are also derived. Finally, simulation results are presented to verify our analytical results.**

***Index Terms*—Line-of-sight, multiple-antenna power transmitter, energy harvesting, outage probability, ergodic capacity, bit error rate.**

I. Introduction

A. Background and motivation

Energy harvesting is an effective means to prolong the life time of wireless devices and perhaps even to enable their battery-free operations. Although scavenging energy from solar power, wind and other sources is feasible, their unreliability is problematic for the provision of quality of service parameters. Thus, wireless power transfer with dedicated power transmitters is an option [1]. Thus, theoretical analysis of energy harvesting (EH) links over fading channels is necessary to gain insights and to quantify exact performance. Most published analyses however focus on Rayleigh and Nakagami-m fading models, which however assume rich-scattering multipath channels without a dominant line-of-sight (LOS) component. On the other hand, the microwave power transfer distance is about 3–15 meters for typical mobile devices, sensors, and tablets [1].

In such short communication links, however, a LOS component can be dominant. Although the Rician fading model is then most appropriate, EH studies for it are limited. For instance, the impact of Rician fading on the performance of dual-hop energy harvesting amplify and forward (AF) relay systems [2].

Alternatively, a hybrid access point (AP) can transmit energy in the downlink and receive data in the uplink (Fig. 1). The single-antenna user harvests energy from the transmissions of the AP and communicates with the AP in the uplink. This mode has been called the harvest-then-transmit protocol [3] and has led to the concept of the wireless-powered communication network (WPCN) [4]. The applications of this model include wireless sensor networks and RF identification networks [4]. A WPCN with a multi-antenna two-way AF relay and the harvest-then-transmit protocol has also been investigated [5]. In order to understand the performance of EH WPCNs over LOS links, this system could be analyzed in detail.

Thus, an analysis of outage probability (OP), ergodic capacity (EC) and bit error rate (BER) of this system is useful. For instance, [4] has derived the average throughput of this system and the optimal energy harvesting time for delay-limited and delay-tolerant transmissions over Rayleigh fading channels. Reference [6] has derived OP, EC and BER of WPCN over generalized $\kappa - \mu$ fading channels.

B. Problem statement and contributions

However, this system has previously been analyzed under the assumption of non-LOS channels only (see [4], [7] for example). As mentioned before, in typical EH scenarios, this assumption may not hold, and the presence LOS components should be considered. Thus, we aim to characterize the performance of the WCPN under LOS channels. Therefore, this paper generalizes the work of [4] to the LOS case and differs from [4], [7] by treating the symbol error rate (SER) of several modulations in detail.

Due to the presence of the LOS channels, the received signal-to-noise ratio (SNR) at the AP is the product of two independent non-central Chi-square variables. The distribution of this product is complicated and is available only as an infinite series [8]. By using this classical result, we exactly analyze the OP, EC and BER of this network. However, the resulting exact expressions are complicated, infinite series. Therefore, we also develop more insightful asymptotic or approximate expressions. Finally, we consider both delay-limited and delay-tolerant modes.

The main contributions are summarized below. For a specific energy harvesting fraction of time, we derive

1) Exact expressions for OP and EC, which characterize delay-limited and delay-tolerant modes.
2) BER for binary phase shift keying (BPSK), binary differential phase shift keying (BDPSK).
3) Throughput-optimal energy harvesting time at high SNR for delay-tolerant transmission.
4) Asymptotic or approximate analyses to gain insights of the delay-tolerant mode, BPSK and BDPSK.

To the best of our knowledge, this is first paper that derives both exact and asymptotic/approximate performance analysis of the considered system.

Notation: For random variable (rv) X, $f_X(\cdot)$ and $F_X(\cdot)$ denote the probability density function (PDF) and cumulative distribution function (CDF). A circularly symmetric complex Gaussian rv with mean μ and variance σ^2 is $\mathcal{CN}(\mu, \sigma^2)$. The gamma function $\Gamma(a)$ is given in [9, Eq. (8.310.1)]; $K_\nu(\cdot)$ is the ν-th order modified Bessel function of the second kind [9, Eq. (8.432)]; $G_{pq}^{mn}\left(z \mid \begin{smallmatrix} a_1 \cdots a_p \\ b_1 \cdots b_q \end{smallmatrix}\right)$ denotes the Meijer G-function [9, Eq. (9.301)]. A non-central Chi-square RV with n degrees of freedom and non-centrality parameter δ is denoted by $\chi_n^2(\delta)$. The central case occurs when $\delta = 0$.

II. System Model

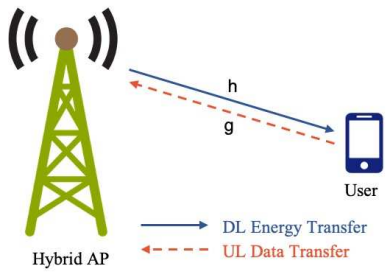

Fig. 1. System Model

Consider the multiple-antenna WPCN with downlink energy transfer and uplink data transmission (Fig. 1). Both the hybrid AP and single-antenna user use half-duplex wireless. The AP is equipped with $n \geq 1$ antennas and uses maximum ratio combiner (MRC) reception for uplink signals. It also performs maximal ratio transmission (MRT) energy beamforming in the downlink, which powers the user. Following [4], [7], we assume the availability of perfect channel state information (CSI) at the AP. The energy transfer channels is denoted as $\mathbf{h} = [h_1, \ldots, h_k, \ldots, h_n]^T \in \mathbb{C}^{n\times 1}$ and the data transfer channel is denoted as $\mathbf{g} = [g_1, \ldots g_k, \ldots, g_n]^T \in \mathbb{C}^{n\times 1}$. The channel coefficients h_k and g_k $(k = 1, \ldots, n)$ are independent and identically distributed (i.i.d.) circularly symmetric complex Gaussian rvs with $h_k \sim \mathcal{CN}(\mu_{k,1}, \sigma_1^2)$ and $g_k \sim \mathcal{CN}(\mu_{k,2}, \sigma_2^2)$. Thus, we can write $\|\mathbf{h}\|^2 = \frac{1}{2}{\sigma_1}^2 X_1$ and $\|\mathbf{g}\|^2 = \frac{1}{2}{\sigma_2}^2 X_2$ where X_i $(i = 1, 2)$ are $\chi_{2n}^2(\lambda_i)$ with non-centrality parameter $\lambda_i = \frac{2}{\sigma_i^2}\sum_{k=1}^{n}|\mu_{k,i}|^2$. The PDF of X_i, $i = 1, 2$, is the non-central Chi-square PDF [8, Eq. (1)].

For a transmission block time T, the user harvests energy for duration τT, and it transmits information for $(1-\tau)T$ where $\tau \in [0, 1]$. Thus, the total harvested energy at the user is $E_h = \eta\tau P\|\mathbf{h}\|^2$ where η is the energy conversion efficiency and P is the transmit power of the AP. Without loss of generality, we assume $T = 1$. Since in the uplink, the received signal at the AP is $y_A = \sqrt{E_h/(1-\tau)}\mathbf{g}s + \mathbf{n}$, where s is the energy-normalized information symbol and $\mathbf{n}$ is the additive white Gaussian noise (AWGN) term. The SNR at the AP can be expressed as

$$\gamma_A = \frac{\tau\eta P\sigma_1^2\sigma_2^2}{4(1-\tau)N_0}\|\mathbf{h}\|^2\|\mathbf{g}\|^2 = \frac{\tau}{1-\tau}\overline{\gamma}X_1X_2, \quad (1)$$

where $\overline{\gamma} = \frac{\eta P\sigma_1^2\sigma_2^2}{4N_0}$ and N_0 is the noise variance. The exact PDF of the product $Y = X_1X_1$ is highly complicated. However, it can be derived via the Mellin transform techniques, and the details can be found in [8, Eq. (11)]. We will indeed exploit this classical result. Since γ_A is simply the product of constant $\frac{\tau}{1-\tau}\overline{\gamma}$ and Y, the PDF of γ_A can be given as

$$f_{\gamma_A}(y) = \sum_{m=0}^{\infty}\sum_{j=0}^{m}\frac{\psi(m,j)(1-\tau)}{e^{\frac{1}{2}(\lambda_1+\lambda_2)}\tau\overline{\gamma}}\left(\frac{y(1-\tau)}{\tau\overline{\gamma}}\right)^{\alpha(m)} \cdot K_{2j-m}\left(\sqrt{\frac{y(1-\tau)}{\tau\overline{\gamma}}}\right), \quad (2)$$

where $K_n(x)$ is modified Bessel function of second kind of order n, $\alpha(m) = n + \frac{m}{2} - 1$ and symbol $\psi(m,j) = \frac{\lambda_1^j\lambda_2^{m-j}2^{1-2n-2m}}{j!(m-j)!\Gamma(n+j)\Gamma(m-j+n)}$. The special case $\lambda_1 = \lambda_2 = 0$ is studied in [4].

A. The Patnaik approximation

The PDF of the product of two non-central Chi-square variables (2) is complicated because it is an infinite series of modified Bessel functions. Also, the averaging of error-rate expressions over $K_n(x)$ Bessel functions is challenging. Although (2) leads to exact results, due to these reasons, numerical issues can arise. Consequently, simpler approximations are desirable. Patnaik [10] suggested approximating a non-central Chi-square rv by a scaled central Chi-square rv.

Following this idea, we take two independent rvs, say, $Z_i \sim \chi_{v_i}^2(0)$, for $i = 1, 2$. We next approximate the two non-central rvs as $X_i \approx c_iZ_i$ where c_i and v_i are to be determined by matching the first two moments of X_i to those of c_iZ_i. Thus, this moment matching yields $c_i = \frac{2n+2\lambda_i}{2n+\lambda_i}$ and $v_i = \frac{(2n+\lambda_i)^2}{2n+2\lambda_i}$.

For the subsequent developments, the following general result proves to be useful.

Proposition 1. *The moment generation function (MGF) of the product of two independent $Z_i \sim \chi_{v_i}^2(0)$, $i = 1, 2$ is given as*

$$M_{Z_1Z_2}(t) = \frac{1}{2^{v_2}t^{\frac{v_2}{2}}}\Psi\left(\frac{v_2}{2}, \frac{v_2-v_1}{2}+1; \frac{1}{4t}\right), \quad (3)$$

where $\Psi(a, b; z)$ is the confluent hypergeometric function [9, Eq. (9.211.4)].

Proof. We begin with the definition of the MGF and find

$$\begin{aligned} M_{Z_1Z_2}(t) &= \mathbb{E}\left[e^{-tZ_1Z_2}\right] \\ &\overset{(a)}{=} \frac{1}{2^{\frac{v_1}{2}}}\mathbb{E}\left[\left(\frac{1}{2}+tZ_2\right)^{-\frac{v_1}{2}}\right] \\ &\overset{(b)}{=} \frac{1}{2^{\frac{v_2}{2}}\Gamma\left(\frac{v_2}{2}\right)}\int_0^\infty \frac{z_2^{\frac{v_2}{2}-1}e^{-\frac{z_2}{2}}}{(1+2tz_2)^{\frac{v_1}{2}}}dz_2 \\ &\overset{(c)}{=} \frac{1}{2^{v_2}t^{\frac{v_2}{2}}\Gamma\left(\frac{v_2}{2}\right)}\int_0^\infty \frac{u^{\frac{v_2}{2}-1}e^{-\frac{1}{4t}u}}{(1+u)^{\frac{v_1}{2}}}du, \end{aligned} \quad (4)$$

where we first fix Z_2 and take average over Z_1 by using the well-known MGF of a central Chi-square rv (Step (a)). By taking the expectation over Z_2, we find the integral expression in Step (b). From the substitution $u = 2tz_2$, we get step (c) and finally (3) via [9, Eq. (9.211.4)]. ∎

III. Performance Analysis

A. Delay-Limited Transmission Mode

1) Exact Analysis: This mode is suitable for user applications that are delay sensitive. The received signal at the AP thus needs to be decoded block by block. The average throughput can be evaluated by obtain OP with a fixed transmission rate R. OP is then given by the probability that the instantaneous throughput, $\log_2(1+\gamma_A)$, falls below a certain threshold γ_{th}

$$\begin{aligned} P_{ave} &= (1-P_{out})\,R\,(1-\tau) \\ &= (1-F_{\gamma_A}\left(2^{\gamma_{th}}-1\right))\,R\,(1-\tau), \end{aligned} \tag{5}$$

where $F_{\gamma_A}(y)$ is the CDF of γ_A and it can be derived as

$$\begin{aligned} F_{\gamma_A}(y) &\overset{(a)}{=} \sum_{m=0}^{\infty}\sum_{j=0}^{m}\frac{\psi(m,j)\,(1-\tau)}{e^{\frac{1}{2}(\lambda_1+\lambda_2)}\tau\overline{\gamma}}\int_0^y\left[\left(\frac{t\,(1-\tau)}{\tau\overline{\gamma}}\right)^{\alpha(m)}\right. \\ &\left.\cdot K_{2j-m}\left(\sqrt{\frac{t\,(1-\tau)}{\tau\overline{\gamma}}}\right)\right]dt \\ &\overset{(b)}{=} \sum_{m=0}^{\infty}\sum_{j=0}^{m}\frac{\psi(m,j)G_{1,3}^{2,1}\left(\frac{y(1-\tau)}{4\tau\overline{\gamma}}\,\middle|\,\begin{matrix}-\alpha\,(m)\\ \frac{2j-m}{2},-\frac{2j-m}{2},-\alpha\,(m)-1\end{matrix}\right)}{2e^{\frac{1}{2}(\lambda_1+\lambda_2)}\left(\frac{\tau}{1-\tau}\overline{\gamma}\right)^{\alpha(m)+1}y^{-(\alpha(m)+1)}} \end{aligned} \tag{6}$$

where $y=2^{\gamma_{th}}-1$. Line (a) follows from the definition of CDF; Line (b) is derived directly from [9, Eq. (6.592.2)].

B. Delay-Tolerant Transmission Mode

1) Exact Throughput Analysis: In this mode, the AP has sufficient buffering capacity and can tolerate the delay for decoding the stored signals together. Therefore, the EC at the AP is the appropriate measure of the throughput. Moreover, since the SU uses τ fraction of time to harvest energy so effective information transmission time fraction is $(1-\tau)$. Thus, the throughput is given by

$$\begin{aligned} C &= (1-\tau)\int_0^{\infty}\log_2\left(1+y\right)f_{\gamma_A}(y)\,dy \\ &\overset{(a)}{=} \sum_{m=0}^{\infty}\sum_{j=0}^{m}\frac{(1-\tau)2^{2\alpha(m)-1}\psi(m,j)}{2\ln(2)e^{\frac{1}{2}(\lambda_1+\lambda_2)}\frac{\tau}{1-\tau}\overline{\gamma}}\int_0^{\infty}\left[G_{2,2}^{1,2}\left(y\,\middle|\,\begin{matrix}1,1\\1,0\end{matrix}\right)\right. \\ &\left.\cdot\,G_{0,2}^{2,0}\left(\frac{y\,(1-\tau)}{4\tau\overline{\gamma}}\,\middle|\,\begin{matrix}\alpha\,(m)\\ \frac{2j-m}{2}+\alpha\,(m),-\frac{2j-m}{2}+\alpha\,(m)\end{matrix}\right)\right]dy \\ &\overset{(b)}{=} \sum_{m=0}^{\infty}\sum_{j=0}^{m}\frac{(1-\tau)2^{2\alpha(m)-1}\psi(m,j)}{\ln(2)e^{\frac{1}{2}(\lambda_1+\lambda_2)}\frac{\tau}{1-\tau}\overline{\gamma}} \\ &\quad G_{2,4}^{4,1}\left(\frac{1-\tau}{4\tau\overline{\gamma}}\,\middle|\,\begin{matrix}-1,0\\-1,-1,\frac{2j-m}{2}+\alpha\,(m),-\frac{2j-m}{2}+\alpha\,(m)\end{matrix}\right). \end{aligned} \tag{7}$$

To derive (7), we express $\ln(1+x)$ and $K_n(x)$ in terms of Meijer G-functions by following [4, Eq. (12)], and then arrive at the above expression of C.

2) Asymptotic Throughput Analysis: We analyze the behaviour of (7) as $\overline{\gamma}\to\infty$. This is described by the following proposition.

Proposition 2. *The asymptotic capacity of the delay tolerant transmission mode is given by*

$$C = \frac{1-\tau}{\ln 2}\left[\ln\overline{\gamma}+D-\ln\left(\frac{1-\tau}{\tau}\right)\right], \tag{8}$$

when $\overline{\gamma}\to\infty$, where $D=\ln c_1+\ln c_2+\psi\left(\frac{v_1}{2}\right)+\psi\left(\frac{v_2}{2}\right)+2\ln 2$ and ψ is Euler psi function [9, Eq. (8.360)], and $\overline{\gamma}=\frac{\eta P\sigma_1^2\sigma_2^2}{4N_0}$.

Proof. Let $C=(1-\tau)C^*$ where

$$\begin{aligned} C^* &= \mathbb{E}\left[\log_2\left(1+\gamma_A\right)\right] \\ &\approx \left[\log_2\frac{\tau}{1-\tau}\overline{\gamma}+\mathbb{E}\log_2\left(X_1\right)+\mathbb{E}\log_2\left(X_2\right)\right] \\ &= \left[\log_2\frac{\tau}{1-\tau}\overline{\gamma}+\mathbb{E}\log_2\left(c_1Z_1\right)+\mathbb{E}\log_2\left(c_2Z_2\right)\right], \end{aligned} \tag{9}$$

when $\overline{\gamma}\to\infty$. We find $\mathbb{E}\left[\log(Z)\right]=\left.\frac{d\mathbb{E}\left[Z^{t-1}\right]}{dt}\right|_{t=1}$. If $Z\sim\chi_v^2(0)$, we find that $\mathbb{E}\left[Z^{t-1}\right]=2^{t-1}\Gamma(t+v/2-1)/\Gamma(v/2)$. ∎

The asymptotic capacity expression (8) can be exploited to obtain a closed-form expression for the optimal energy harvesting-time fraction τ^* at high SNR. The derivation is similar to Appendix B [4] and is omitted. We find that

$$\tau^* \approx \frac{1}{1+W\left(\overline{\gamma}e^{D-1}\right)}, \tag{10}$$

where the Lambert function satisfies $W(x)\,e^{W(x)}=x$, and $W(x)$ is monotonically increasing for $x\geq 0$.

C. Average Bit Error Rate

This can be evaluated directly by averaging the conditional bit error rate, $P_e(y)$ [11], i.e., $\bar{P}_{BER}=\int_0^{\infty}P_e(y)\,f_{\gamma_A}(y)\,dy$ where $f_{\gamma_A}(y)$ is the PDF of γ_A.

1) Exact BER of BPSK: This modulation is robust against noise and widely used in mobile standards. The conditional BER of BPSK is given in [11, Eq. (8)]. By using that result, we find that

$$\begin{aligned} \bar{P}_{BER} = \sum_{m=0}^{\infty}\sum_{j=0}^{m}\frac{a\psi(m,j)\,(1-\tau)}{be^{\frac{1}{2}(\lambda_1+\lambda_2)}\tau\overline{\gamma}\sqrt{\pi}}2^{2\alpha(m)-1}\cdot \\ G_{2,3}^{2,2}\left(\frac{1-\tau}{4b\tau\overline{\gamma}}\,\middle|\,\begin{matrix}0,-\frac{1}{2}\\ \frac{2j-m}{2}+\alpha\,(m),-\frac{2j-m}{2}+\alpha\,(m),-1\end{matrix}\right), \end{aligned} \tag{11}$$

where $a=\frac{1}{2}$ and $b=1$.

2) Approximate BER of BPSK:

$$\begin{aligned} \bar{P}_{BER,app} &= \mathbb{E}\left[a\mathrm{erfc}\left(\sqrt{\mathrm{b}\gamma_{\mathrm{A}}}\right)\right] \\ &\overset{(a)}{=} \mathbb{E}\left[\frac{a}{\pi}\int_{-\frac{\pi}{2}}^{\frac{\pi}{2}}\exp\left(-\frac{b\gamma_A}{\sin^2\theta}\right)d\theta\right] \\ &\overset{(b)}{=} \frac{a}{\pi}\int_{-1}^{1}\frac{\mathbb{E}\left[\exp\left(-\frac{b\gamma_A}{t^2}\right)\right]}{\sqrt{1-t^2}}dt \\ &\overset{(c)}{=} \frac{a}{\pi}\int_{-1}^{1}\frac{M_{Z_1Z_2}\left(\frac{u}{t^2}\right)}{\sqrt{1-t^2}}dt \\ &\overset{(d)}{=} \frac{a}{w}\sum_{k=1}^{w}M_{Z_1Z_2}\left(\frac{u}{t_k^2}\right), \end{aligned} \tag{12}$$

where (a) is a well-known expression of $\operatorname{erfc}(\cdot)$; (b) is due to the substitution $\sin\theta = t$; (c) is because of using the Proposition 1., $u = \frac{\tau}{1-\tau}\overline{\gamma}c_1c_2$; (d) follows from the Gauss-Chebyshev quadrature rule [12, eq. (1)], $t_k = \cos\left(\frac{(2k-1)\pi}{2w}\right)$ and w is the number of nodes used.

3) Exact BER of BDPSK: For this modulation, conditional BER is given by $P_e(y) = ae^{-by}$. In this case, the BER can be derived via the MGF technique [13], [14]. Fortunately, the MGF of γ_A can be derived via [11, eq. (4)]. Thus $\bar{P}_{BER}$ can be derived as

$$\bar{P}_{BER} = \sum_{m=0}^{\infty}\sum_{j=0}^{m} \frac{a\psi(m,j)\,(1-\tau)^{\alpha(m)+\frac{1}{2}}}{2e^{\frac{1}{2}(\lambda_1+\lambda_2)}\,(\tau\overline{\gamma})^{\alpha(m)+\frac{1}{2}}}\Delta e^{\frac{1-\tau}{8(\tau\overline{\gamma})}} \cdot W_{-\alpha(m)-\frac{1}{2},\frac{2j-m}{2}}\left(\frac{1-\tau}{4\tau\overline{\gamma}}\right), \tag{13}$$

where, $\Delta = \Gamma\left(\alpha(m)+j-\frac{m}{2}+1\right)\Gamma\left(\alpha(m)-j+\frac{m}{2}+1\right)$; $W_{\lambda,\mu}(\cdot)$ [9, Eq. (9.220)] is the Whittaker function. For BDPSK, $a = \frac{1}{2}$ and $b = 1$.

4) Approximate error analysis of BDPSK: Although (13) can be computed precisely, it is an infinite series. A simpler BER expression can be more useful sometimes. To that end, we use the Patnaik approximation (Section II. A). Accordingly, we get $\bar{P}_{BER,app} = \mathbb{E}\left[ae^{-b\frac{\tau}{1-\tau}\overline{\gamma}X_1X_2}\right] = \mathbb{E}\left[ae^{-uZ_1Z_2}\right]$, where $u = b\frac{\tau}{1-\tau}\overline{\gamma}c_1c_2$. Thus, we find

$$\bar{P}_{BER,app} = \frac{a}{2^{v_2}u^{\frac{v_2}{2}}}\Psi\left(\frac{v_2}{2}, \frac{v_2-v_1}{2}+1; \frac{1}{4u}\right). \tag{14}$$

The accuracy of this expression (14) will be verified next.

IV. Numerical and Simulation Results

The analytical derivations are validated via Monte-Carlo simulations. We set transmission unit block time T is 1 and noise variance $\sigma_1^2 = \sigma_2^2 = 1$. The exact results given in infinite series are evaluated as follows. We write $W_m = \sum_{m=1}^{m} Q_i$, $W_0 = 0$ and $W_m = W_{m-1} + Q_m$. When $\frac{Q_m}{W_m} \leq 0.01$, the series computation stops.

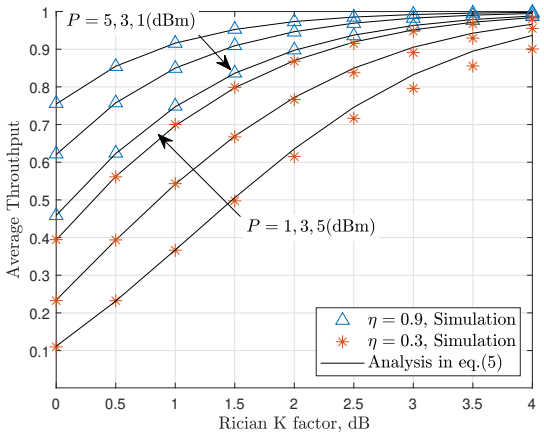

Fig. 2. Average Throughput of delay-limited mode versus K for $\tau = 0.4$, $\lambda_1 = \lambda_2 = K$, $N = 4$, and $\gamma_{th} = 1$ dBm.

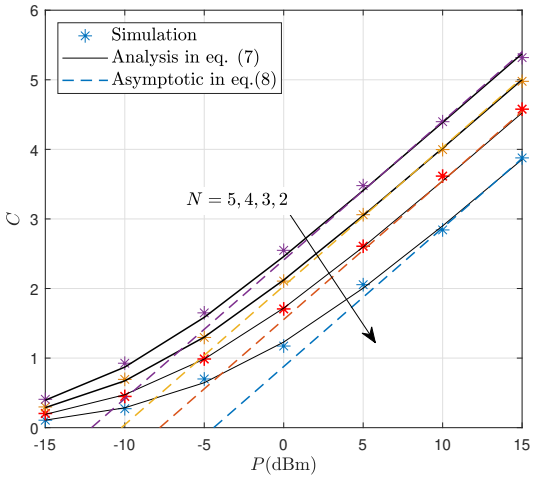

Fig. 3. Average Throughput of delay-tolerant mode versus P for $\eta = 0.9$, $\tau = 0.4$ and $\lambda_1 = \lambda_2 = 2$.

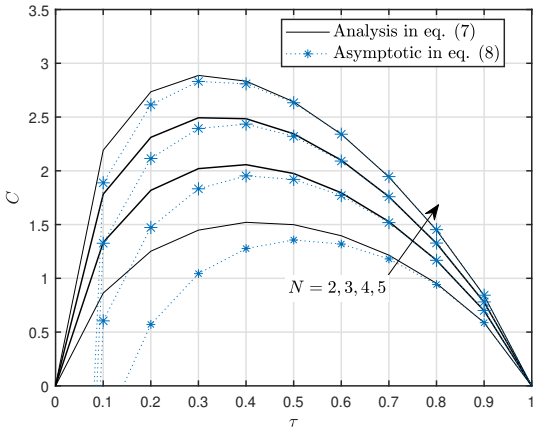

Fig. 4. Average Throughput of delay-tolerant mode versus τ for $\eta = 0.9$, $P = 1$ dBm and $\lambda_1 = \lambda_2 = 1.5$.

Fig. 2 shows the delay-limited average throughput curves of the LOS network versus the Rician K factor with different transmit powers at the AP and energy conversion efficiency at the user. The analysis results tightly coincide with simulation results, which verified the correctness of (5). Rician channel K factor is the ratio between the power in the direct path and the power in the other, scattered, paths. And $K = 0$ represents Rayleigh fading, and $K \to \infty$ is equivalent to no fading. The delay-limited average throughput is improved with increasing Rician K factor. Unsurprisingly, larger energy conversion efficiency and transmit power improve performance. The user is then able to harvest more energy during the downlink phase, and thus has more power available during the in uplink phase.

Fig. 3 shows the average throughput of the delay-tolerant mode versus the transmit power of the AP. Although the asymptotic curves (8) diverge from the exact ones (7) when transmit power is low, rapid convergence occurs with the increase of transmit power. The throughput performance improves with either increasing the transmit power or increasing the number of antennas at the AP. Also, the simulation results

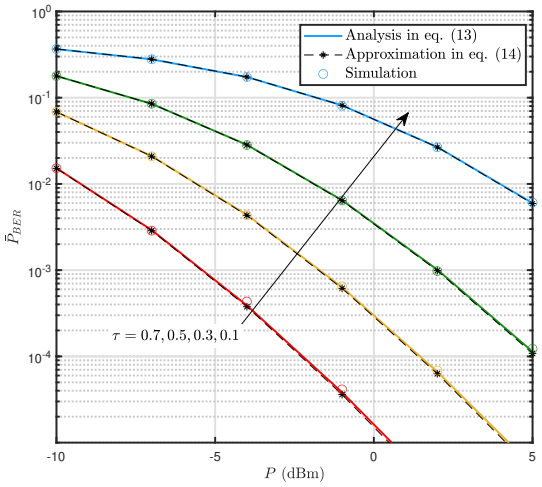

Fig. 5. $\bar{P}_{BER}$ of BDPSK versus P for $n = 5$, $\eta = 0.9$ and $\lambda_1 = \lambda_2 = 2$.

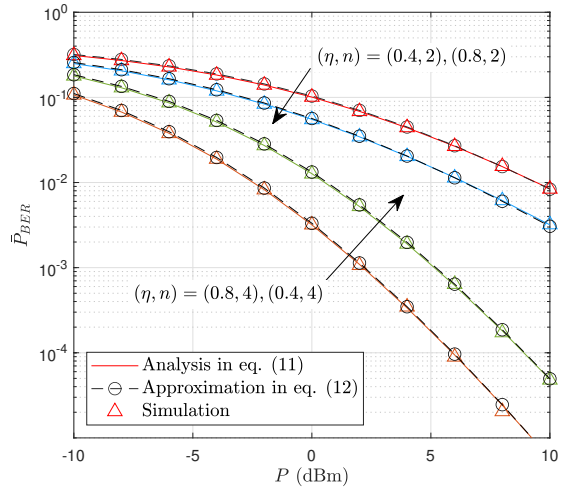

Fig. 6. $\bar{P}_{BER}$ of BPSK versus P for $n = 5$, $\tau = 0.4$ and $\lambda_1 = \lambda_2 = 1$.

match exact ones tightly.

Fig. 4 plots the throughput versus energy harvesting time for the delay-tolerant mode with different numbers of AP antennas. The figure shows throughput-optimal energy harvesting times for different antenna numbers, confirming the analytical result (10). Since the user harvests energy for time fraction τ and transmits information for $(1 - \tau)$, optimal τ^* balances these two activities best. Convergence of asymptotic curves (8) to the exact ones (7) occurs when the energy harvesting time and the number of antennas at the AP increase.

The BERs of BDPSK and BPSK versus the transmit power of the AP are plotted in Fig. 5 and Fig. 6, respectively. Note that the trifecta of exact analysis, simulations and approximations coincide nicely. This close match validates the correctness of (11) and (13) and confirms that the Patnaik central Chi-squared approximation (Proposition. 1) works well. As well, these two figures confirm the trend that the BER improves with the increasing transmit power at the AP. Larger transmit power at the AP means the user can receive signals with larger SNR, which improves the quality of the communication link. As expected, larger energy harvesting time improves the BER since the user has larger power budget in the uplink. Moreover, Fig. 6 shows that the BER of BPSK is improved as either the number of antennas or energy harvesting efficiency increases.

V. Conclusion

A comprehensive performance analysis of energy beamforming in a WPCN over LOS channels has hitherto been lacking. We remedy this gap by analyzing the WPCN (Fig. 1), which consists of a multiple-antenna AP and a single-antenna, battery-less user device. It will harvest energy from the downlink AP transmissions and the sends data to the AP. We derived exact and approximate/asymptotic expressions for OP, EC and BER. They were validated via Monte-Carlo simulations.

Our main findings can be summarized as follows:

1) OP, EC and BER can be improved by increasing transmit power P and the number of AP antennas.
2) When the channel K factor is large (strong LOS), the system performance improves. Interestingly, the optimal harvesting time fraction is insensitive to the K factor.

References

[1] K. Huang and X. Zhou, "Cutting the last wires for mobile communications by microwave power transfer," *IEEE Wireless Commun. Mag.*, vol. 53, no. 6, pp. 86 – 93, June 2015.

[2] H. Ding and D. B. Costa, "On the effects of LOS path and opportunistic scheduling in energy harvesting relay systems," *IEEE Trans. Commun.*, vol. 15, no. 12, pp. 8506–8524, Dec. 2016.

[3] L. Liu and R. Zhang, "Multi-antenna wireless powered communication with energy beamforming," *IEEE Trans. Wireless Commun.*, vol. 62, no. 12, pp. 4349–4361, Dec 2014.

[4] W. Huang, H. Chen, Y. Li, and B. Vucetic, "On the performance of multi-antenna wireless-powered communications with energy beamforming," *IEEE Trans. Veh. Technol.*, vol. 65, no. 3, pp. 1801–1808, Mar. 2016.

[5] A. Salem and K. A. Hamdi, "Wireless power transfer in multi-pair two-way AF relaying networks," *IEEE Trans. Commun.*, vol. 64, no. 11, pp. 4578–4591, 2016.

[6] N. Deepan and B. Rebekka, "On the performance of wireless powered communication networks over generalized κ- μ fading channels," *Physical Communication*, vol. 36, p. 100759, 2019.

[7] Z. Chang, S. Zhang, and Z. Wang, "Energy efficient optimisation for large-scale multiple-antenna system with WPT," *Communications IET*, vol. 12, no. 5, pp. 552–558, 2018.

[8] W. T. Wells, R. L. Anderson, and J. W. Cell, "The distribution of the product of two central or non-central Chi-square variates," *The Annals of Mathematical Statistics,*, vol. 33, no. 3, pp. 1016–1020, Sep. 1962.

[9] I. S. Gradshteyn and I. M. Ryzhik, *Table of Integrals, Series, and Products, 7th edition*. Academic Press, 2007.

[10] P. B. Patnaik, "The non-central χ^2 and F distributions and their applications," *Biometrika*, vol. 36, no. 1, pp. 202–232, June 1949.

[11] P. Bithas, N. C. Sagias, P. T. Mathiopoulos *et al.*, "On the performance analysis of digital communications over generalized-K fading channels," *IEEE Commun. Lett.*, vol. 10, no. 5, pp. 353–355, May 2006.

[12] Y. Dhungana and C. Tellambura, "Rational Gauss-Chebyshev Quadratures for wireless performance analysis," *Wireless Commun. Letters, IEEE*, vol. 2, no. 2, pp. 215–218, April 2013.

[13] C. Tellambura, "Evaluation of the exact union bound for trellis-coded modulations over fading channels," *IEEE Trans. Commun.*, vol. 44, no. 12, pp. 1693–1699, 1996.

[14] C. Tellamura, A. Annamalai, and V. Bhargava, "Closed form and infinite series solutions for the MGF of a dual-diversity selection combiner output in bivariate Nakagami fading," *IEEE Trans. Commun.*, vol. 51, no. 4, pp. 539–542, 2003.